

# EXPLORATION OF A NOVEL PLATE ANCHOR GEOMETRY WITH A VIEW TO REDUCING MATERIAL USAGE

Angus Dyson<sup>1</sup>, Matthew Bennett<sup>2</sup> and Pierre Rognon<sup>3</sup>

<sup>1,2</sup>Research Assistant, <sup>3</sup>Senior Lecturer,

Particles and Grains Laboratory, School of Civil Engineering, The University of Sydney, NSW, 2006, Australia.

## ABSTRACT

Soil anchors are often used to stabilise structures. Various anchor designs have been developed with the aim of achieving higher pull-out capacity at lower cost. Examples include plate, helical, grouted and drilled shaft anchors. Presented herein is a series of experiments investigating the anchoring properties of root-like fractal shapes. The pull out resistance and resilience (pull-out resistance after an initial displacement) of a plate anchor with a root-like shape in a model granular soil comprising 50µm glass beads is compared to that of a plain plate anchor. Results show that such root-like shapes are characterised by a higher pull-out resistance per unit volume of anchor material, and a higher resilience than plain shape anchors.

By focusing on a particular anchor shape in a model soil, this study pinpoints the potential benefit of using complex shape anchors. These results pave the way for further investigations of various anchors shapes, for instance fractal, wheel or mesh geometries, aiming at finding the shape that optimise the pull-out resistance and resilience.

## 1 INTRODUCTION

Soil anchors have been used to stabilise structures for thousands of years. Modern construction of transmission towers, utility poles, submerged pipelines, tunnels and offshore structures rely on effective and cost efficient strategies for soil anchoring (Das 2012; Liu et al. 2012). Existing strategies include plate anchors (which are the focus of this study), direct embedment anchors, helical anchors, grouted anchors, anchor piles and drilled shafts. Installation of plate anchors involves excavating soil down to a desired depth, installing the anchor, backfilling and compacting (Figure 1a). Plate anchors are usually circular, rectangular or long strips, and made using concrete, steel or timber. The quality of anchoring is characterized by the pull out resistance  $F_0$ , which is the maximum tensile force the anchor can sustain before the soil fails and let it move upward irreversibly.

Several models have been developed to predict the pull-out resistance of shallow anchors as a function of their size and depth. These models all consider that the pull-out resistance is governed by the weight of the soil that would be mobilized when the anchor moves upward (Murray and Geddes 1987; Cheuk et al. 2008; Niroumand and Kassim 2010; Liu et al. 2012; Jung et al. 2013). They differ however, in the estimation of the volume of mobilized soil, delineated by a failure envelope. For a circular anchor of diameter  $D$ , cylinders (Majer 1955; Meyerhof and Adams 1968), truncated cones (Downs and Chieuzzi 1966; Veesaert and Clemence 1977) and circular (Baker and Kondner 1966) failure envelopes have previously been proposed (see Figures 1b,c). In any case, the pull-out force can be generally expressed as:

$$F_0 = \rho g A H f(\theta) \tag{1}$$

where  $\rho$  is the density of the soil,  $H$  the anchor depth,  $g$  the gravity,  $A$  the anchor surface area in the pull-out direction, and the function  $f$  accounts for the shape or the failure envelope, defined by a characteristic angle  $\theta$ . The shape function is 1 for a cylindrical failure envelope. For a truncated cone failure envelope, it is greater than one and can be expressed as:

$$f(\theta) = \frac{1}{3} \left( 1 + 2 \frac{H}{D} \tan(\theta) \right)^2 + 2 \frac{H}{D} \tan(\theta) \tag{2}$$

The value of  $\theta$  is usually within the range  $2/3\phi < \theta < \phi/2$  where  $\phi$  is the soil friction angle.

As a consequence, there are two basic solutions to improve the pull-out resistance of such anchors, burying them deeper or making them larger. However, these two solutions require larger excavations and/or larger amount of material to build the anchor, which increases the construction cost. A third solution is to combine multiple plates spaced along the vertical axis. However, the increase in pull-out force saturates when plates get too close to each other due to a screening effect (Kouzer and Kumar 2009; Kumar and Sahoo 2011). A fourth solution, which is the focus of this study, is to design the anchor shape to improve its anchoring properties.

In this paper, a particular type of anchor shape is investigated, that is inspired tree's root system. The primary role of the tree's root systems is to access nutrients in soil. Another role of roots, equally critical to the tree's survival, is to ensure that the tree can resist wind loading. As a consequence, it is possible that root geometries may present interesting anchoring abilities, which could be used in geotechnical applications. To probe this hypothesis, a set of pull-out experiments of fractal shape anchors were carried out in a model granular soil. Experiments will focus on the anchor pull-out resistance and on their resilience, i.e., their pull-out resistance after an initial displacement.

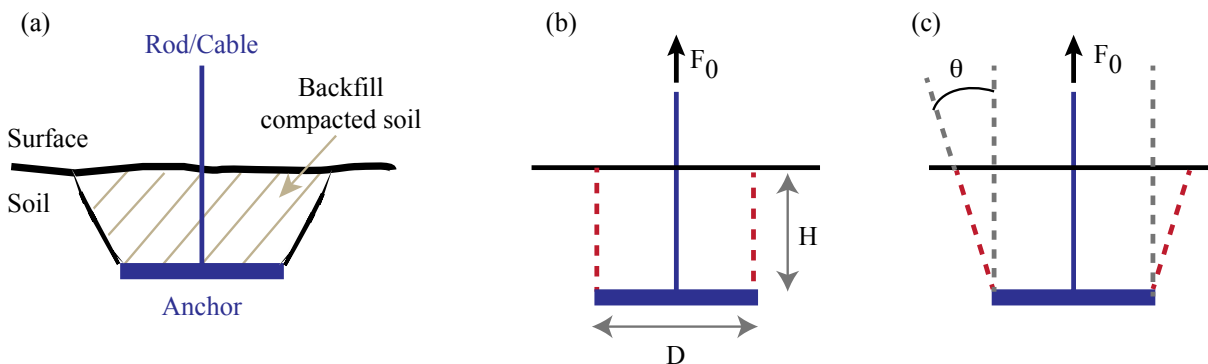


Figure 1. Soil anchoring using shallow plate anchors: (a) schematic of practical setting; illustration of cylinder (b) and cone (c) failure envelopes (red dashed lines) from which existing models deduce the anchor pull-out force  $F_0$  (see Equation (1)).

## 2 PULL-OUT EXPERIMENTS OF FRACTAL ANCHORS

To highlight the effect of the anchor geometry, we have designed a model experimental configuration illustrated in Figure 2. The model soil is comprised of small spherical glass beads of diameter ranging from 50  $\mu\text{m}$  to 60  $\mu\text{m}$ . This model soil is characterised by a relatively low friction angle,  $\phi = 21^\circ$ . The advantage of using this model soil is that it reaches its maximum density  $\rho = 2300 \text{ kg/m}^3$  irrespective of the mode of preparation. Experiments can then easily be repeated in the same conditions.

The model soil is confined in a square glass tank with 40cm width. An anchor is buried in the soil and connected to a linear stage and a force meter via a shaft of diameter 10mm.

### 2.1 EXPERIMENTAL PROTOCOL

Each experiment starts with a similar preparation step, which consists in emptying the tank, placing the anchor at a desired depth  $H$ , and filling the tank with the glass beads. At this stage, the anchor is subjected to a non-null, relatively small tension force that slightly varies from test to tests depending on the filling process. The value of that initial force did not affect the measured pull-out resistance.

Experiments then consist of lifting the anchor upward at a prescribed velocity  $V^{up}$ , and measuring the tension force as a function of the displacement.

### 2.2 ANCHOR DESIGN

We designed two types of anchors, namely plain disks and planar fractals (see Figure 2b,c). The two anchors have the same outer diameter,  $D = 8\text{cm}$ , and are 4mm thick. They feature a 4mm hole in their centre to fit the shaft connection. Fractal anchors are comprised of six first-generation branches joining in the centre, with a relative angle of  $60^\circ$ . Each sub-generation comprises two sister branches forming an angle of  $60^\circ$ . The branches length decrease by a factor of 1.8 from one generation to another.

The design of this fractal anchor was performed by a recursive algorithm able to produce a stereo lithographic 3D model, which was then 3D-printed. This fractal anchor can be characterized by its surface ratio  $\phi$ :

$$\phi = \frac{A^{\text{Root}}}{A^{\text{Disk}}} = 0.47 \quad (3)$$

where  $A^{\text{Root}}$  is the surface area of the fractal anchor and  $A^{\text{Disk}} = \pi D^2/4$  is the surface area of the disk of same diameter. Given that the anchors have the same thickness, the surface ratio  $\phi$  directly quantifies how much material is needed to build the fractal anchor as compared to the full disk.

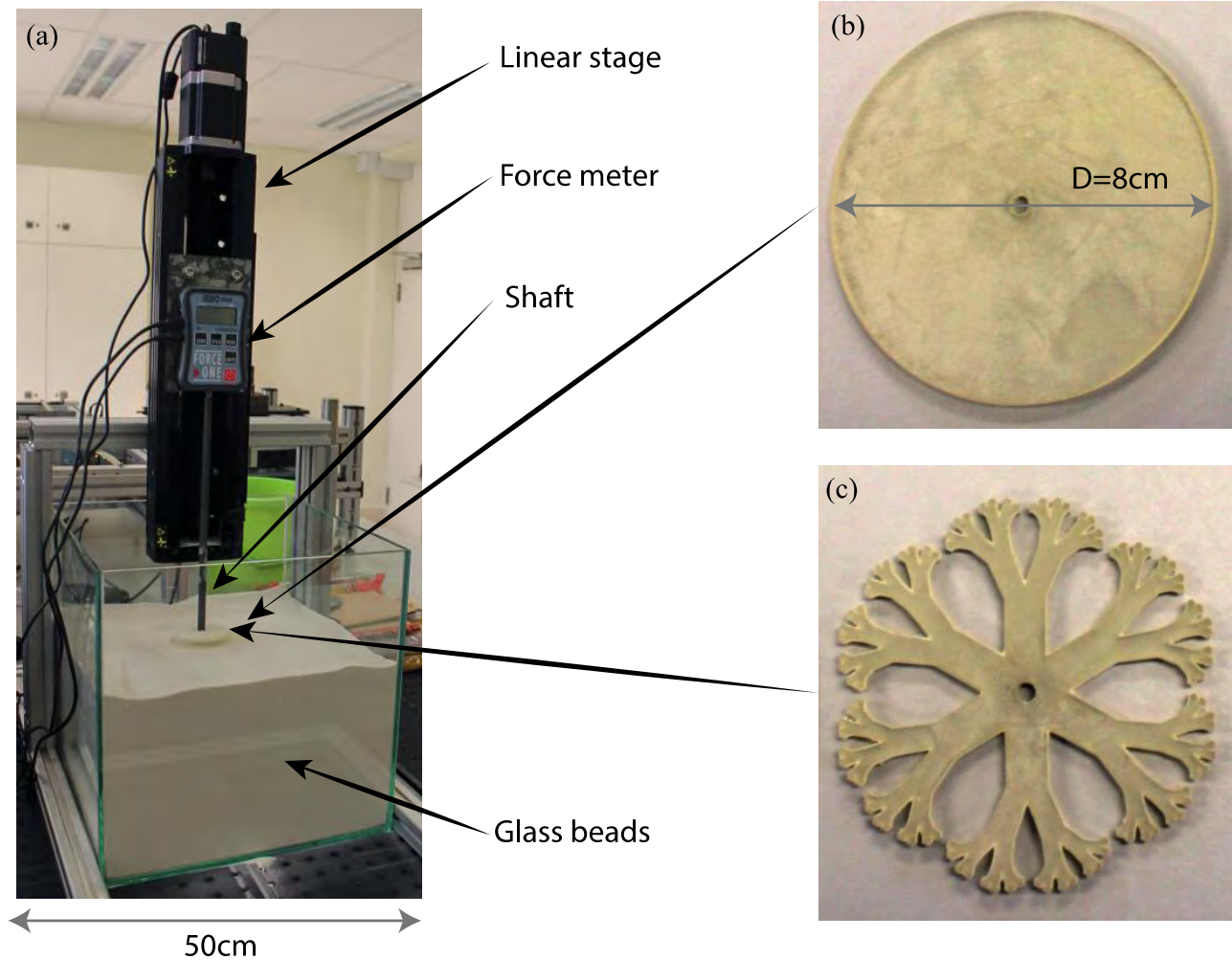


Figure 2. (a) Experimental device to measure the pull-out force; (b) plain disk and (c) fractal anchors.

### 3 PULL-OUT FORCE

#### 3.1 DISK ANCHOR

Figure 3a shows the force  $F(z)$  measured by the force meter while pulling out a disk anchor. Initially, the anchor is at a depth  $z=H$ . As the linear stage lifts up the anchor, the force rapidly builds up and reaches a maximum, and then slowly decreases as the anchors get closer to the free surface,  $z=0$ . The pull-out force  $F_0$  is defined as the maximum force on such a curve.

We have checked that the value of  $F_0$  is not affected by the proximity of lateral walls, as long as they are farther than a few centimetres from the anchor edge. We have also checked that the value of  $F_0$  is not too sensitive to the mode of preparation: experiments can be reproduced with a variation in  $F_0$  lesser than 5%. Finally, we varied the velocity of

pulling  $V^{up}$  between 1mm/s and 20cm/s with no noticeable effect on  $F_0$ . Note that the non zero value of the force at the free surface,  $F(z=0)$ , is due to the formation of a static pile on top of the anchor.

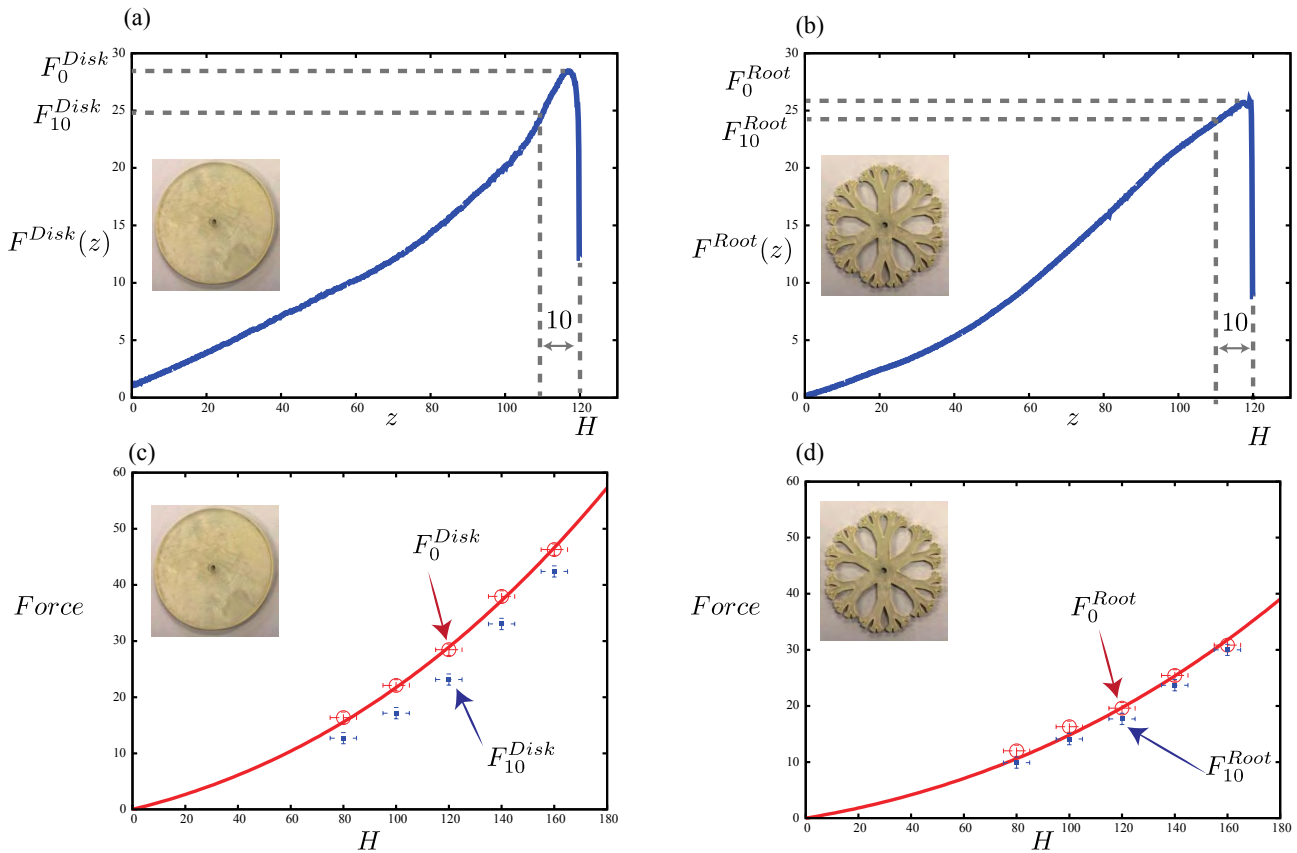


Figure 3. Pull-out force for disk and fractal anchors. Force versus depth  $z$  as the anchor moves toward the surface ( $z=0$ ) from its initial position ( $z=H=120mm$ ): (a) disk anchor and (b) fractal anchor. Maximum pull-out force  $F_0$  as a function of the initial depth  $H$ : (c) disk anchor and (d) root anchor. (c,d) Each symbol represent on test, error bars account for the force meter accuracy of 1N and the non-uniformity of the free surface of the order of 5mm; red lines represents the model described by Eqs. (1), (2) and (4) (see text for more details). (a-d) forces are expressed in Newtons and distances in millimetres.

**3.2 FRACTAL ROOT ANCHOR**

Figure 3b shows the force measured while pulling-out a fractal anchor, starting from the same depth  $H=120mm$ . The force  $F(z)$  exhibits a shape similar to that of the disk anchor. However, the value of the pull-out force is lower.

**3.3 DEPTH EFFECT**

Similar experiments were repeated for both anchors for different depths ranging from 80mm to 160mm, which corresponds to  $H/D$  ranging from 1 to 2. Results of the pull-out force  $F_0$  are showed for the disk anchor on Figure 3c. On this Figure, the prediction of the model described in Eq. (1) and (2) is represented by the red line. The density of the glass beads was measured,  $\rho = 2300 \text{ kg/m}^3$ , the surface area of the anchor is known,  $A = \pi D^2/4 = 50.2 \text{ cm}^2$  and the best fit of the data was obtained with an angle  $\theta = 13.2^\circ$ . Note that this value is consistent with the range  $2/3\phi < \theta < \phi/2$  that the friction angle of the glass beads is  $\phi=21^\circ$ . The quality of the fit shows that the cone failure envelope model is able to capture our results.

Figure 3d shows the results obtained with the fractal anchor. The red line was obtained using Eqs. (1) and (2), also with  $\rho = 2300 \text{ kg/m}^3$  and  $\theta = 13.2^\circ$ , and considering the anchor surface area  $A^{Root} = \phi \pi D^2/4 = 23.6 \text{ cm}^2$ . However, a prefactor  $\alpha = 1.47$  needs to be introduced as a fitting parameter to capture the data. Hereafter,  $\alpha$  will be referred to as *shape factor*. The pull-out force of the fractal anchor is then captured by a modified version of the model in Eqs. (1) and (2):

$$F_0^{Root} = \alpha \rho g A^{Root} H f(\theta) \tag{3}$$

Let us now use these results to compare the pull-out force of a fractal anchor and of a disk anchors made using the same amount of material, i.e., with the same surface area. The pull-out force of the fractal anchor would be  $\alpha=1.47$  times higher than the pull-out resistance of the plain disk.

### 4 RESILIENCE

The pull-out experiment results showed in Figures 3a,b show the behaviour of the anchoring force once the anchor has moved past the failure point, as illustrated in figures 2 a,b. For both disk and fractal anchors, the force then drops as the anchor moves upward. The drop seems to be more important for the disk anchor than for the fractal anchor. It can be quantified by the following quantity:

$$Res = 100 * \frac{F_0 - F_{10}}{F_0} \tag{4}$$

where  $F_{10}$  is the anchoring force after an anchor displacement of 10 mm (see Figures 3a,b).  $Res$  thus measures the percentage of anchoring force after an anchor displacement of 10 mm, relative to the pull-out force. It can be seen as a measure of the anchor resilience, which characterises its pull-out resistance after an initial displacement past the failure point. Large value of  $Res$  would correspond to a large force drop and a low anchor resilience.

Figure 4 shows the disk and fractal anchors' resilience as a function of the initial depth  $H$ . The disk anchor loses up to 22% of its force for shallow depth, a value that decreases for deeper anchors. The fractal anchors systematically exhibit much lower value of  $Res$ , and thus a much better resilience.

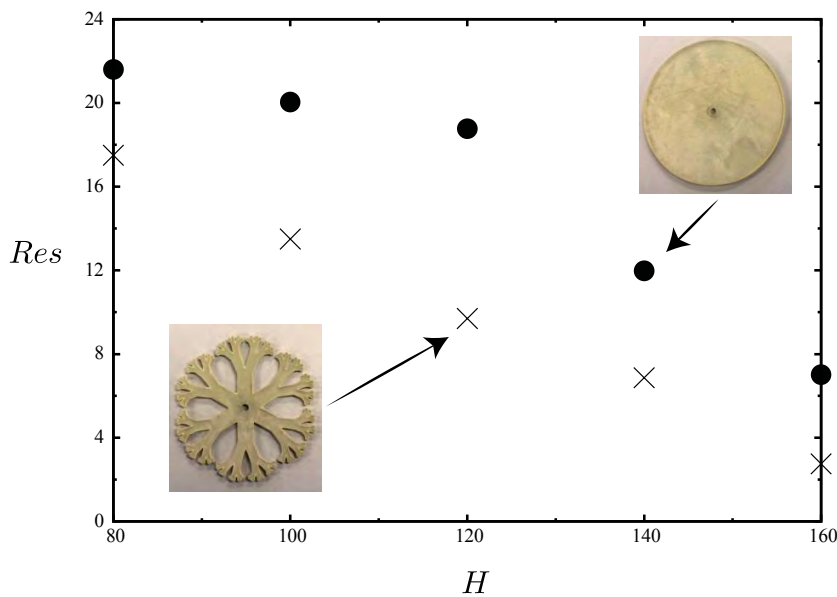


Figure 4. Resilience (%) of disk (circle) and fractal (cross) anchors as a function of the depth  $H$  as defined in equation (4).

### 5 CONCLUSION

The experimental results we presented here indicate that fractal root-inspired anchors have interesting anchoring properties in granular soils. Results show that their pull-out resistance can be described by a cone-failure envelope model if a shape factor  $\alpha$  is introduced. Focusing on one fractal shape anchor, we obtained a shape coefficient of 1.47, which means that using the same amount of material, a fractal shape would have a superior pull-out-resistance than a plain disk.

Further still, these anchors were found to exhibit interesting resilience properties, represented by the loss in anchoring resistance after the anchor has moved past the failure point. Results showed that fractal anchors are significantly more resilient than plain disk anchors.

These results constitute a first proof of concept suggesting that that complex shape anchors may be an interesting solution for geotechnical applications requiring optimum use of material and high anchor resilience. They pave the way for further investigations of complex anchor geometries, both 2D and 3D, aiming at identifying the shapes that optimise the pull-out resistance, the resilience and the required amount of material. Beyond fractal shapes, other shape such as wheel or mesh shapes may exhibit interesting anchoring properties.

To determine the optimum anchor shape, future work should focus on identifying the relevant geomechanical mechanisms controlling the anchor mechanical response, including soil deformation pattern near the anchor, and mechanisms of arching that may lead to clogging the anchor holes.

## 5 REFERENCES

- Baker, W. H., & Konder, R. L. (1966). "Pullout load capacity of a circular earth anchor buried in sand". *Highway Research Record*, (108).
- Clemence, S. P., & Veesaert, C. J. (1977, January). "Dynamic pullout resistance of anchors in sand". In *Proceedings of the International Symposium on Soil-Structure Interaction, Roorkee, India* (pp. 389-397).
- Cheuk, C. Y., White, D. J., & Bolton, M. D. (2008). "Uplift mechanisms of pipes buried in sand". *Journal of geotechnical and geoenvironmental engineering*, 134(2), 154-163.
- Das, B. M. (2012). *Earth anchors*. Elsevier.
- Downs, D. I., & Chieurrzi, R. (1966, April). "Transmission tower foundations". In *Electric Power@s Today and Tomorrow* (pp. 335-390). ASCE.
- Kouzer, K. M., & Kumar, J. (2009). "Vertical uplift capacity of two interfering horizontal anchors in sand using an upper bound limit analysis". *Computers and Geotechnics*, 36(6), 1084-1089.
- Kumar, J., & Sahoo, J. P. (2011). Upper bound solution for pullout capacity of vertical anchors in sand using finite elements and limit analysis. *International Journal of Geomechanics*, 12(3), 333-337.
- Jung, J. K., O'Rourke, T. D., & Olson, N. A. (2013). "Uplift soil-pipe interaction in granular soil". *Canadian Geotechnical Journal*, 50(7), 744-753.
- Liu, J., Liu, M., & Zhu, Z. (2012). "Sand Deformation around an Uplift Plate Anchor". *Journal of Geotechnical and Geoenvironmental Engineering*, 138(6), 728-737.
- Majer, J. (1955). "Zur berechnung von zugfundamenten". *Osterreichische Bauzeitschrift*, 10(5), 85-90.
- Meyerhof, G. G., & Adams, J. I. (1968). "The ultimate uplift capacity of foundations". *Canadian geotechnical journal*, 5(4), 225-244.
- Murray, E. J., & Geddes, J. D. (1987). "Uplift of anchor plates in sand". *Journal of Geotechnical Engineering*, 113(3), 202-215.
- Niroumand, H., & Kassim, K. A. (2010). "Analytical and numerical study of horizontal anchor plates in cohesionless soils". *Electronic Journal of Geotechnical Engineering*, 15, 1-12.